Journal of Thermal Analysis Vol. 46 (1996) 809-832

Dedicated to Professor Bernhard Wunderlich on the occasion of his 65th birthday

SLOW CALORIMETRY AND HEAT OF FUSION OF POLY(4-METHYL PENTENE-1)

H. Phuong-Nguyen, G. Charlet and G. Delmas*

Université du Québec à Montréal, Département de Chimie, C.P. 8888, succ. Centre-Ville Montréal, Québec H3C 3P8

*Université Laval CERSIM Cité Universitaire, Sainte-Foy, Québec G1K 7P4, Canada

Abstract

The heat of fusion of nascent poly(4-methyl pentene-1)(P4MP) has been measured with a slow temperature-ramp. Two melting ranges have been observed. A broad endotherm is found mostly below the equilibrium melting temperature, $T_{m,o}$. The total heat of fusion ΔH_{total} is the sum of ΔH_{dsc}, the melting enthalpy found by rapid heating and a second endotherm, $\Delta H_{network}$, a contribution associated with the heat of disordering of a physical network. Similar reported analysis have been presented before on polyethylene and isotactic polypropylene. The ΔH_{total} for P4MP is found to be 100±10 J g^{-1}, in the upper range of the expected values of ΔH_o, the heat of fusion of perfect crystals. The value of ΔH_{total} constitutes a lower limit of ΔH_o in cases like that of P4MP where other methods lead to ambiguous results. The comparison of T_m and T_d, the melting and dissolution temperatures, and other results support the hypothesis that the equilibrium phase at the melting of P4MP is partially rigid while it is a liquid (or a mixture of a glass and a liquid) at the dissolution.

Keywords: enthalpy, perfect crystals, poly(4-methyl pentene-1), slow calorimetry, strain dissolution, strain melting

Introduction

Poly(4-methyl pentene-1)(P4MP1) is an interesting polyolefin that can be synthetized with a high degree of stereoregularity. The conditions of its synthesis and its properties have been described in a recent review [1]. It crystallizes easily from the melt to a triclinic crystal with four chains in the unit cell. The chains have a helical conformation with seven monomers for two helical turns in the more stable conformation of modification I. From solution, large single crystals are obtained [2, 3], the temperature of crystallization determining if they are of the more stable structure, or one of two others whose crystalline parameters are also known [4–7].

An unusual feature of P4MP is the low density of its crystals that are, below 50 °C, lighter than the non-crystalline phase. P4MP has a large expansion coef-

0368–4466/96/ $ 5.00

John Wiley & Sons, Limited
Chichester

ficient, so that the specific volume of a sample increases considerably from room temperature (*RT*) to its melting temperature T_m (245°C). At T_m, the change of volume on fusion is small (0.05 $cm^3\ g^{-1}$) [8, 9] compared to that of PE (0.2 $cm^3\ g^{-1}$). There are indications that the order-disorder transition is not complete at T_m, some association between the helicoidal chains persists in the melt [10–12]. A recent X-ray study [13] has shown that high pressure leads to a disordered phase at (*RT*) with the intermediate of a liquid-crystalline phase.

Viscosity and calorimetry on dilute solutions in low molecular weight solvents give evidence of chain association [14–16]. More concentrated solutions in low molecular weigth solvents form gels [4–7, 14–19] on cooling. These gels are stable above the dissolution temperature, T_d, of the crystals. In some solvents, the gel persists up to T_d +70 K. Above T_d, the gels show no X-ray crystallinity. The origin of the cohesive junctions in these gels, particularly in those formed at the first dissolution, has been the object of extensive investigations. The finding of an exothermic heat of swelling [14] over a range of temperature below T_d and the stability of the gel in highly expanded solvents (above the normal boiling point) gives support to the hypothesis of favorable packing arrangement between the chains and the solvent molecules [14–15].

Crystallinity

The homopolymer from ICI used in this laboratory has an X-ray crystallinity of 0.77 [16, 21] which is consistent with its high NMR stereoregularity [21]. For other polyolefins (polyethylene (PE), isotactic polypropylene (iPP)), the evaluation of crystallinity by density, α_c (*d*) is reliable, and α_c (*d*) is usually consistent with α_c (X-ray). The review cited above summarizes the difficulties in evaluating the crystallinity of P4MP from different techniques. They are associated with the characteristics mentioned above, namely the rather small difference in specific volume between the crystalline, v_c, and the amorphous phase, v_a, either at *RT* or in the melt at T_m. For instance using the thermodynamics relationship and the same value for the variation of T_m with pressure (dT_m/dP), three research groups found a large range of ΔH_o (the heat of fusion of perfect crystals) namely 117 J g^{-1} [22], 87 J g^{-1} [16, 21] and 60 J g^{-1} [9] because they used different values of v_c–v_a at T_m.

Calorimetric crystallinity

For semi-crystalline polyolefins, the lower value of α_c (*H*) obtained from the ratio of ΔH_{exp} to ΔH_o has been recognized and associated with incomplete melting [23–24]. The new technique of slow DSC [25–31], i.e. measuring the melting endotherm over a long time period, increases the value of ΔH_{exp} and brings α_c (*H*) closer to α_c (*d*), within the restrictions mentioned below. For P4MP, the ambiguity in α_c (*H*) is not resolved by slow calorimetry because of the uncertainty in the value of ΔH_o.

In the present paper we report results of slow calorimetry. The work was initiated to bring some clarification about the P4MP crystallinity. Before giving the results for P4MP, a characterization of slow calorimetry will be presented based on experiments on PE and iPP.

The technique of slow calorimetry

This technique has been made possible when the SETARAM C80 calorimeter became available in our laboratory a few years ago. It was used initially to understand gel formation in polyethylene solutions [26], where it was found that dissolution of the polymer occurs in two steps: one with a fast and one with a very slow kinetics. The slow kinetics was associated with the existence of a network present in the gel and the fast kinetics with the dissolution of crystals. The process with the fast kinetics is detectable by fast DSC, the process with the slow kinetics not. It needs the presented data obtained by slow calorimetry. The interest in slow calorimetry grew when it was discovered that two processes with different kinetics existed also in slow melting traces and that the effect seems to be a general feature of semi-crystalline polymers. The network is situated in the non-crystalline phase and has enough short-range order to be meltable on measurement with a slow heating-ramp.

A typical trace derived on slow melting is given in Fig. 1. The range of melting is large. It may reach 100–120 K if the T ramp is 3 K h^{-1}. Two effects lead

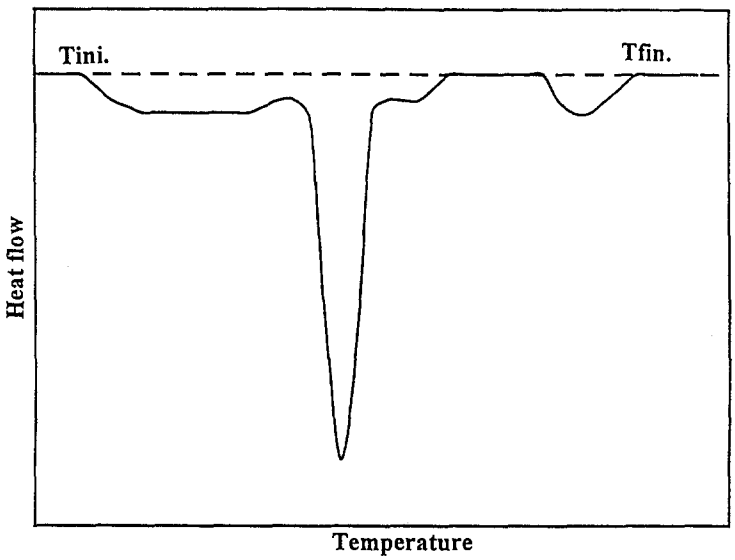

Fig. 1 Schematic representation of the melting trace of a semi-crystalline polyolefin by slow calorimetry. The new result is the endotherm at high temperature with a slow kinetics. It is associated with the disordering of a physical network. Depending on the polymer and its history, the position of the flat endotherm is displaced below or above the main endotherm. A region of arrested melting is seen between the two endotherms

to the large ranges of melting temperature for flat endotherms: first, the heterogeneity of the network in terms of density of entanglements and second, the expansion of the material. This expansion in a system where the chains are linked by entanglements leads to strain and an increase of the melting temperature. A range of temperature where melting is arrested, as shown in Fig. 1, is a frequent occurrence in PE samples.

An endotherm with a slow kinetics has been observed in chemically crosslinked PE samples [31], the melting range of which is similar to that of the physical network.

Integration between $T_{initial}$ and T_{final} permits to evaluate the total heat of fusion:

$$\Delta H_{total} = \Delta H_{dsc} + \Delta H_{network} \quad (1)$$

The integration of the main peak gives ΔH_{dsc}, the heat of fusion obtained by the usual technique of fast DSC.

For polymers for which ΔH_o is known, such as PE and iPP, it was found that $\Delta H_{total} = \Delta H_o$. This result is surprising even for linear PE or highly stereoregular iPP. It means that the loss of long-range order occurred by the entangled chains and does not significantly affect the cohesion between chains. Cooling a macromolecular liquid below the crystallization temperature, T_c, lowers its enthalpy by the amount ΔH_o which is relatively insensitive to the amount of short-range and long-range order induced by the cooling. The substitution of long-range order for short-range order does not eliminate the order-disorder transition, but changes its kinetics sufficiently to make it unrecognizable by fast DSC. Further reflexion is needed to understand the non-cooperative part of the change in enthalpy in a semi-crystalline polymer.

Although there is some uncertainty about ΔH_{total} because of the large temperature range of integration, the findings that were obtained for a variety of conditions have a solid basis, as shown from the research on several polyolefins in bulk or in solution. The technique of slow calorimetry which adds the contribution $\Delta H_{network}$ to the change of enthalpy on melting, is thought to be able to give new information on ΔH_o of P4MP crystals.

The existence of complex morphology with entangled interlamellar chains or tie-molecules, similar to the phase called here the network phase, has been known in semi-crystalline polyolefins and investigated by different techniques. For P4MP, swelling and electronic microscopy [32, 34] and other methods [32–38] have been used to probe the relations between the phases in the sample.

The melting or dissolution of the network fractions is often incomplete. This is due to the fact that the expansion brings large strains to some densely crosslinked and strained regions, so that some crystals do not melt. By changing the conditions, such as increasing the maximum temperature, by changing the rate

of heating or using a substrate, one can bring the melting to completion, using as indicator the value of ΔH_{total}.

In the present paper, the results of slow melting of nascent and recrystallized P4MP are presented. The reversibility of the melting trace is illustrated by the slow crystallization traces given. A reevaluation of the value of ΔH_o by the techniques using phase equilibrium will be done in the light of the new results of slow calorimetry. Two dissolution traces are added to confirm the optical determination of T_d by calorimetry [21].

Experimental

Polymer

The sample of P4MP is the same as in previous studies (ICI, Welwyn Garden Hertfordshire, England). It is a nascent highly stereoregular homopolymer sample made of small globules of 200 μ average diameter. The characterization by ^{13}C NMR, X-ray and DSC was reported [4–7, 16].

Solvents

They were reagent grade from Aldrich and used as received.

Apparatus

The sensitive and stable SETARAM C80 calorimeter was used. It can accommodate large size cells and be rotated while making a dissolution experiment. The base line fluctuations are between 5 and 10 μW for a slow heating/cooling rate (v=1–3 K h^{-1}).

Integration and base line substraction

A complete balance of reference and sample cells, and of the thermocouples, cannot be achieved. As the imbalance is amplified by the temperature ramp, the base line is slanted between 30 and 280°C [25–31]. In order to improve the presentation of the results and reduce subjectivity of the analysis, the base line is calculated for each trace using points outside the regions with deviations of the heat flow situated at temperatures below the beginning and above the end of the endotherms. After substraction, integration is made by planimetry of the curve.

Procedure

The sample (20–100 mg) is placed in a glass tube (OD=15mm) for melting of the neat polymer, or polymer mixed with a substrate, or with a solvent for dissolution experiments. After elimination of air with a current of dry N_2 or by

applying a vacuum, the tube is sealed and placed in the calorimeter to stabilize at the temperature of the beginning of the temperature ramp. The initial temperature of the calorimeter varied between 60 and 100°C for the meltings and 30 and 50°C for the dissolutions. The time to reach equilibrium is usually 17 h. Equilibrium is reached in about 3–4 h. However, to be in the best conditions to analyse small deflections from the base line, the sample was left overnight i.e. about 17 h before starting the temperature-ramp. This procedure has the advantage of adding a controlled annealing time to the sample history.

Substrate

For melting experiments (without solvent), the substrate is Hg, fine glass beads, or a finely divided stainless steel powder, or the polymer itself. It has been found [25] that the melting of nascent iPP (and of nascent PE) is more complete in presence of a substrate. An explanation was given in terms of a phase separation between network and main crystals initiated by adsorption on the solid. The phase separation takes the role of reducing the strain on the chains and making melting more complete. Although there are difference in the traces when the polymer melts by itself or on the substrate, this point has not been investigated thoroughly for this paper.

Recrystallized samples

The polymer is crystallized in the calorimeter from the melt with a temperature-ramp (3 K h^{-1}) which starts at 280°C. The main peak indicates that the polymer crystallizes between 239 and 226°C, the exotherm having a sharp maximum at 230.5–232°C. The temperature ramp is then continued down to 60°C .

The melt has the following history: i. the nascent polymer is placed directly into the calorimeter at 280°C for 17 h or ii. It is the result of a temperature ramp between 60 and 280°C at 3 K h^{-1}. In the second history there is no additional isothermal residence time at 280°C.

The value of T_c in a given temperature-ramp is an indication of the kinetics of crystallization. In the slow temperature-ramp used, T_c is independent of the substrate. This is not the case of iPP whose T_c can be raised by 15–20 K by different substrates [25].

Temperature stability

P4MP seems to be chemically stable over the complete temperature-ramp. No exotherm is recorded on the traces.

T_d measurements

The values of the dissolution temperature T_d are those measured under the microscope [21]. In a series of solvents, the calorimetric dissolution trace at in-

creasing temperature has been obtained. The temperature of the high- temperature side of the main peak of dissolution is taken as T_d (calorimetric). It corresponds within one or two K to the measurement under the microscope.

X-ray crystallinity: short- and long-range order

The value of α_c by fast DSC, slow calorimetry, and X-ray diffraction were compared, although they do not measure the same order. In the text, short-range order and long-range order are distinguished with their corresponding contributions to ΔH_{total}. However, the distinction between long- and short-range order is not clear-cut. The intensity of the X-ray pattern is determined mainly by the large-size crystallites, but the small crystals increase α_c (X-ray) by their diffraction by a non-negligible amount. These small crystals melt in the low-T region of the endotherms, on the same temperature range as do the lesser-strained network crystals. In the division of the enthalpy made in the tables, they have not been included in ΔH_{dsc} which is obtained by integration between a narrow temperature interval (233–250°C), but they are included in the enthalpy obtained from fast DSC whose integration interval is 206–247°C. In order to permit a comparison between the values of α_c (H) of the two temperature ramps and of those with α_c (X-ray), part of $\Delta H_{network}$ should be included. By adding $1/2\Delta H_{network}$ to ΔH_{dsc} to calculate α_c (slow calorimetry), one finds α_c (slow calorimetry) comparable to α_c (X-ray), as is shown in Table 1. Similar analyses have been done on iPP.

Results and discussion

The results will be presented in three parts. In the first part, the data leading to the evaluation of ΔH_o are given. In the second part, the hypothesis that P4MP melts with strain and dissolves with a reduced strain, is presented with justifications. The data of T_d in many solvents are reevaluated. In the last part, the different traces of melting/crystallization and dissolution of P4MP are analyzed.

A. The measurement of ΔH_{total} and of ΔH_o

Table 1 gives the values of the total change of enthalpy, ΔH_{total}, and of its two components, ΔH_{dsc} and $\Delta H_{network}$, for three successive measurements: The melting of the nascent sample, its crystallization, and the second melting of the recrystallized samples (noted as $n=1$–3). The details are listed in Tables 2–4, with references to selected figures, shown below.

The data are the average of five or six measurements made under different conditions. The value of ΔH_{total} increases from 79 to 102 J g^{-1} between $n=1$ and $n=3$. The enthalpy corresponding to the long-range order, ΔH_{dsc}, increases in

Table 1 Average values of the change of enthalpy of P4MP

	ΔH_{total} /J g^{-1}	ΔH_{dsc} /J g^{-1}	$\Delta H_{network}$/J g^{-1}	α_c $(H)^b$	α_c $(H)^c$
Melting nascent[a]	79	49	30	0.49	0.64
Crystallization[a]	92	46	46	0.46	0.69
Second melting[a]	102	55	47	0.55	0.79

[a] Average of 5 or 6 measurements

[b] with ΔH_{dsc}

[c] with $\Delta H_{dsc} + 0.5\ \Delta H_{network}$ (see the experimental part)

the second melting by about 10%, but $\Delta H_{network}$ changes the most between the first and the second melting, from 30 to 47 J g^{-1}. This result is interpreted as the effect of the long residence at high temperature, associated with the three temperature ramps at 3 K h^{-1}. This treatment permits the fusion of the order in the network.

By analogy with results on PE and iPP and considering the experimental data of Table 1, the value of the lower limit of ΔH_o is taken to be about 100 J g^{-1}.In the following text, it will be proposed that melting is complete (C) when ΔH_{total} is near ΔH_o. Otherwise, it is taken to be incomplete (I).

The next part will present an explanation of the apparent failure of the Flory-Huggins equation in giving ΔH_o from T_d values.

B. Non-equilibrium phase-changes for P4MP

Melting in equilibrium with a glass and dissolution in equilibrium with a liquid.

Non-equilibrium melting has been conceptually well described [40] and investigated mostly on PE. Non-equilibrium dissolution has hardly been studied. Without solvent, non-equilibrium phase-changes can occur in different modes. One is the well-known case of lamellar thickening during fusion which raises T_m by several degrees. Thickening occurs less in solution because of a slower rate of recrystallization and a lower dissolution temperature. Another mode of non-equilibrium melting has been observed when crystals melt in the presence of a strained melt. The strained melt has itself several origins: one can be external and due to physical restrained imposed on the crystals during melting. Another is internal and caused by a physical network or high values of the rotational barriers between conformations. Whatever the origin, the limited conformational changes lead to strain within the chains. When this situation exists, the non-crystalline phase present in the sample, or produced on melting, stays in a glass-like state up to and above the melting point. A strained melt has an increased T_m because of its higher free energy. Figure 2 is a schematic representation of the changes in the melting trace with the state of the melt. Figure 2a is an example of melting with low strain in the melt that leads to a low value of T_m. The endotherm is relatively broad because of some rearrangement of the melt. Figure 2b is an example of fusion in presence of strained melt, with a high T_m and a narrow peak, indicative of no reorganization. Figure 2c is an example of the overlapping of the two modes. The enthalpy of the narrow peak diminishes in Fig. 2c for the benefit of the lower temperature one. The analysis of melting and dissolution of P4MP leads to the hypothesis that dissolution occurs as shown in Fig. 2a or Fig. 2c and melting as in Fig. 2b. However, the low-temperature endotherms in Figs 6 and 7, below, could be interpreted as melting with a partially relaxed melt (Fig. 2c).

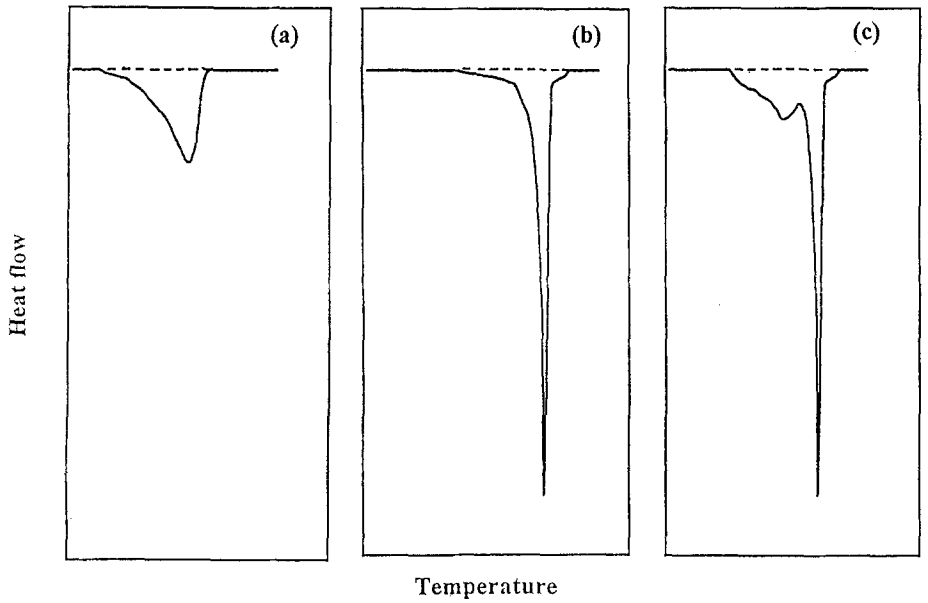

Fig. 2 Schematic representation of melting for different conditions of the melt. 2a. Near equilibrium melting (with a low T_m, but a broadening of the peak due to some reorganization during melting). 2b. Non-equilibrium melting with a high T_m (the narrow melting peak is indicative of no rearrangement during melting). 2c. Intermediate melting (the two endotherms correspond to a combination of cases 2a and 2b)

The justifications of the hypothesis of strain-melting for P4MP are the following :

i. Uncertainty in the assignment of T_g for P4MP and existence of incomplete glass-liquid transition.

ii. Changes below T_m of a semi-crystalline sample, as measured by different heating rates $v(T)$ or by other techniques.

iii. Properties of swollen P4MP (Drawability and heats of swelling).

iv. Thermodynamics of dilute solution.

i. The value of T_g for P4MP is not known with certainty. Literature values range between 18 and 65°C. The lateral groups inhibit free movements in the chain. The increase of mobility for iPP, a less hindered polymer than P4MP, has been shown [41] to occur in stages, in part at T_g and in part between T_g and the beginning of the endotherm of fusion. It would not be surprising if a polymer with longer side groups, like P4MP, had a wider spread of T_g with a delayed end of denitrification. Note that in the case of P4MP, complete relaxation of the melt must require more than a slow change in temperature. The value of T_m is unchanged between DSC and the slow calorimetry experiments, in spite of the extensive disordering ($\Delta H_{network}$) which occurs at low temperature.

ii. Several data reported in the literature can be interpreted as indicators of a continuous glass transition between RT and T_m and also of order left in the melt. The specific volume of the sample increases fast below T_m [8]. Annealing above 200°C [31] changes the morphology of the crystals and indicates a considerable translational mobility of the polymer chains below T_m. During annealing, the unit cell dimensions are unchanged [21, 33], which means that there are some large crystals left to contribute to the X-ray diagram. The response to wetting by a solvent and analysis of mobility by NMR [32] indicates that the mobile fraction increases with temperature. The complex multilayer and interconnected crystals observed by microscopy [33] may be the origin of the high proportion of network crystals which melt below T_m.

iii. An indication that the melt of the non-crystalline part of P4MP can lower its energy in the presence of a solvent is given by the heats of swelling [14]. In *n*-heptane for example, for which $T_d = 124$°C [21], $\Delta H_{swelling}$ is -2.8 J g^{-1} at 25°C and -8 J g^{-1} at 75°C. These figures lead to large values if counted in proportion of the fraction of the polymer which can absorb the solvent. Part of the $\Delta H_{swelling}$ comes from the heats of mixing of two liquids with a different coefficient of expansion. However, the free volume term does not contribute significantly since its numerical value of amorphous polymer has been calculated from equation of state theories to be -1.8 J g^{-1} for heptane [14]. The negative sign of $\Delta H_{swelling}$ could have another origin: the solvent has induced the relaxation of the non-crystalline fraction of P4MP which releases heat by reaching lower free energy states. One would expect the T_m of swollen P4MP to be lowered if the present hypothesis is right. Melting traces have been obtained on swollen polymers and one sees, indeed, that the temperature of the beginning of melting is very low and the peaks very wide. Traces are complex, however, since at higher temperature, the endotherm of fusion, $\Delta H_{network}$, adds to the negative $\Delta H_{swelling}$. These data will not further be commented on. A compelling evidence of the effect of a solvent on T_g is given by the results of the mechanical properties of swollen P4MP samples. While the bulk sample can be drawn only little without breaking, the samples swollen in benzene swell by 480% [34].

Another indication of the transformation of the non-crystalline fraction in the presence of the solvent is the value of ΔH_{total} for the dissolution traces. As written in Table 5, $\Delta H_{network}$ has been reduced or even eliminated when the swollen polymer is dissolved using a temperature ramp, so that ΔH_{total} is less than 70 J g^{-1}.

iv. Thermodynamics of dilute solution

The P4MP crystals are undoubtedly soluble at lower temperatures than expected. For instance, in *n*-pentane, P4MP crystals are soluble at 102°C (i.e. 143 K below T_m) in spite of the large contribution to χ, the polymer-solvent in-

teraction parameter. In cyclopentane, T_d is 30°C, (i.e. 215 K below T_m). The generalty low T_d suggests that its origin lies more in the polymer itself than in the solvent-polymer interaction.

The well known Flory-Huggins model of a polymer solution permits to relate the solution properties to those of the solid by writing that, at T_d, the increase of the chemical potential of the melt between T_m and T_d is exactly compensated by the lowering due to the formation of a polymer solution. In Eq. (2) below

$$\Delta H_u(1-T_d/T_m) = (1-\chi)R(T_d/V_1)V_u \quad (2)$$

ΔH_u is the heat of fusion per unit, V_1 and V_u are the volume of the solvent and the volume of the polymer unit. When the T_d is evaluated for a group of 39 non-polar solvents with the same value of χ (0.4), $\Delta H_u/V_u$ is found 57 J cm^{-3} and $\Delta H_o=(1/d)$ $(\Delta H_u/V_u)$ is 68 J g^{-1} [21], a value intermediate between the high (110 J g^{-1}) and low one (60 J g^{-1}).

The T_d values have been obtained also by calorimetry. If the end of the main dissolution is used as T_d (calorimetry), the T_d reported previously are verified. Attempts have been made to take in Eq. (2) into account that than is a non homogeneous state of the solution after T_d. But such corrections by reducing the lowering of the chemical potential in solution, lead to a still lower value of ΔH_o.

The low value of ΔH_o can be corrected if a relaxed T_m value is introduced in Eq. (2) which becomes:

$$\Delta H_u(1-T_d/T_{m,\,relaxed}) = (1-\chi)R(T_d/V_1)V_u \quad (3)$$

where $T_{m,\,relaxed}$ means that T_m is in equilibrium with a relaxed melt.

The relaxation brought about by the solvent will depend on its size or free volume. In order to quantify the relaxation introduced by the solvent, $T_{m,\,relaxed}$ has been calculated assuming that the right hand side of Eq. (3) is correct with $\chi=0.4$. The values of T_m for relaxed samples lies between 200 and 250°C for the series of the *n*-alkanes when a high value for ΔH_o ($\Delta H_u/V_u=80$ J g^{-1} i.e. $\Delta H_o=95$ J g^{-1}) is used in Eq. (3). These data have been plotted in Fig. 3 against T_d/V_1, for the linear alkanes (o), the cycloalkanes (•) and tridodecylamine (■). As could have been expected, the value of $T_{m,\,relaxed}$ tends towards T_m as the size of the solvent increases. The points with $T_{m,\,relaxed}$ inferior to 100°C correspond to the cycloalkanes where a χ parameter lower than 0.4 is reasonable and contributes to decrease $T_{m,\,relaxed}$.

C. Analysis of the melting and crystallization traces

In the next paragraphs, the detailed analysis of the different calorimetric traces will be given. There are interesting points, not detectable in Table 1 (which only summarizes the tendency of ΔH_{total} and its constituents with thermal history).

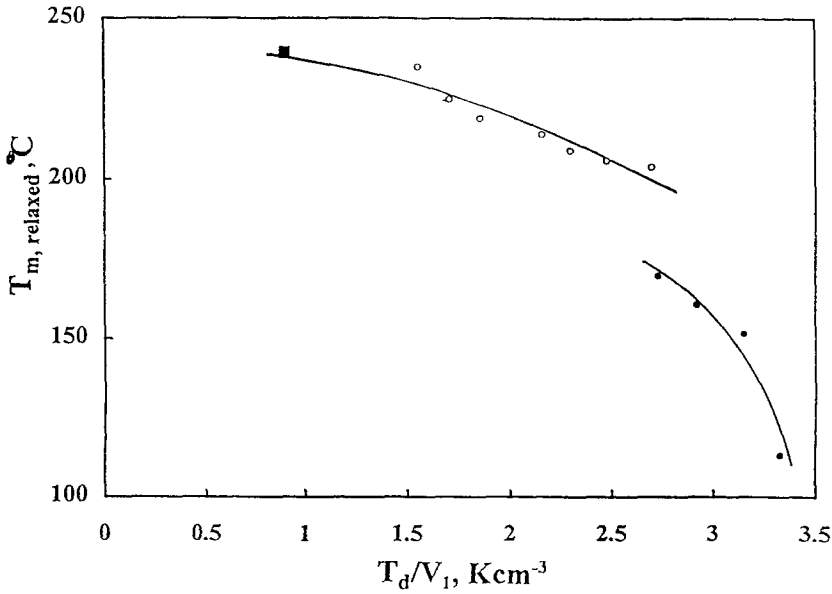

Fig. 3 Calculated values of $T_{m,relaxed}$ from Eq.(3) and the experimental values of $T_{d,\chi}=0.40$ and $\Delta H_o=95$ J g^{-1}. Solvents: (o) *n*-alkanes, (•) cycloalkanes and (■) tridodecylamine. The value of $T_{m,relaxed}$ is an indication of the relaxation of the melt which increases as the molecular size of the solvent diminishes. The cycloalkanes which give gels that melt around 110°C show a distinctly different behavior

In the different columns of Tables 2–4 the following information is given: substrate, weight of polymer (mg), temperature ramp in K h^{-1}, and values of T_m/T_c and ΔH_{total}. The two components of ΔH_{total}, $\Delta H_{network}$ and $\Delta H_{triclinic}$ are given subsequently. The temperature intervals during which these heats evolve are written under the values for $\Delta H_{network}$ and ΔH_{dsc}. The interval is narrow for ΔH_{dsc} and very large for $\Delta H_{network}$.

The data are presented in inverse chronological order: melting of the recrystallized sample is discussed first, then its crystallization from the melt is given, followed by the melting of the nascent. The inverse order underlines the differences in ΔH_{total} between the nascent and recrystallized sample.

1. Trace of melting of a slowly crystallized sample

The trace presented in Fig. 4 illustrates the findings of slow melting, namely the two kinetics of melting and the large value of ΔH_{total}. It shows a flat endotherm starting at 165°C and finishing above T_m (267°C). The position of the endotherm in relation to T_m gives an indication of the strain. The part of the flat endotherm is below 235°C corresponds to the melting of unstrained crystals and the part above 250°C, to the melting of strained crystals. The values of

Table 2 Characteristics of the melting traces of P4MP crystallized in a slow T-ramp

Substrate	m_p / mg	n	v/ K h^{-1}	T_m/ °C	ΔH_{total} / J g^{-1}	$\Delta H_{network,L-T}$ / J g^{-1}	$\Delta H_{network,H-T}$ / J g^{-1}	ΔH_{dsc}/ J g^{-1}	Fig.
Itself	99.8	3	3	247.4	97	28	16	53	7a
					(C)	(108–233)	(159–276)	(233–249)	
Itself	101.7	3	3	245.2	100	64	0	36	7b
					(C)	(198–236)		(236–247)	
Glass beads	66.3	3	3	246.0	94	30	8	56	
					(C)	(146–233)	(249–271)	(233–249)	
Glass beads	66.5	3	3	244.6	122	80	0	42	
					(C)	(129–238)		(238–247)	
Glass beads	113.4	3	3	246.4	90	20	10	60	4
					(C)	(165–235)	(250–267)	(235–250)	
Stainless steel	94.9	5	3	245.8	97	38	0	59	
					(C)	(123–233)		(233–250)	

Table 3 Characteristics of the crystallization traces of P4MP

Substrate	m_p / mg	n	v/ K h^{-1}	T_c / °C	ΔH_{total} / J g^{-1}	$\Delta H_{network,H-T}$ / J g^{-1}	$\Delta H_{network,L-T}$ / J g^{-1}	ΔH_{dsc} / J g^{-1}	Fig.
Itself	99.8	2	3	232.8	107	64		43	
					(C)	(229–100)		(235–229)	
Itself	101.7	2	3	232.0	65	35		30	
					(I)	(229–87)		(236–229)	
Glass beads	66.3	2	3	232.2	85	30	5	50	
					(C)	(223–122)	(256–238)	(238–223)	
Glass beads	66.5	2	3	230.5	97	50	0	47	
					(C)	(226–197)		(239–226)	
Glass beads	77.5	2	3	231.6	101	43	22	36	
					(C)	(228–196)	(263–237)	(237–228)	
Glass beads	113.4	2	3	231.5	76	22	8	46	
					(I)	(228–133)	(267–235)	(235–228)	
Stainless steel	94.9	4	3	231.0	95	40	7	48	5
					(C)	(227–171)	(265–237)	(237–227)	

Table 4 Characteristics of the melting traces of the nascent P4MP

Substrate	m_p / mg	n	v/ K h^{-1}	T_m/ °C	ΔH_{total} / J g^{-1}	$\Delta H_{network,L-T}$ / J g^{-1}	$\Delta H_{network,H-T}$ / J g^{-1}	ΔH_{dsc} / J g^{-1}	Fig.
Itself	51.7	1	1.2	247.3	88	5	33	50	
					(C)	(240–242)	(249–275)	(242–249)	
Itself	99.8	1	12	248.2	57	10	0	47	
					(I)	(150–231)		(231–254)	
Itself	101.7	1	3	246.7	65	20	0	45	
					(I)	(137–236)		(236–250)	
Hg	26.2	1	12	244.0	80	40	0	40	6a
					(I)	(109–226)		(226–253)	
Glass beads	113.4	1	6	246.8	64	16	0	48	
					(I)	(167–233)		(233–253)	
Stainless steel	94.9	1	3	245.7	95	24	8	63	6b
					(C)	(146–228)	(251–268)	(228–251)	

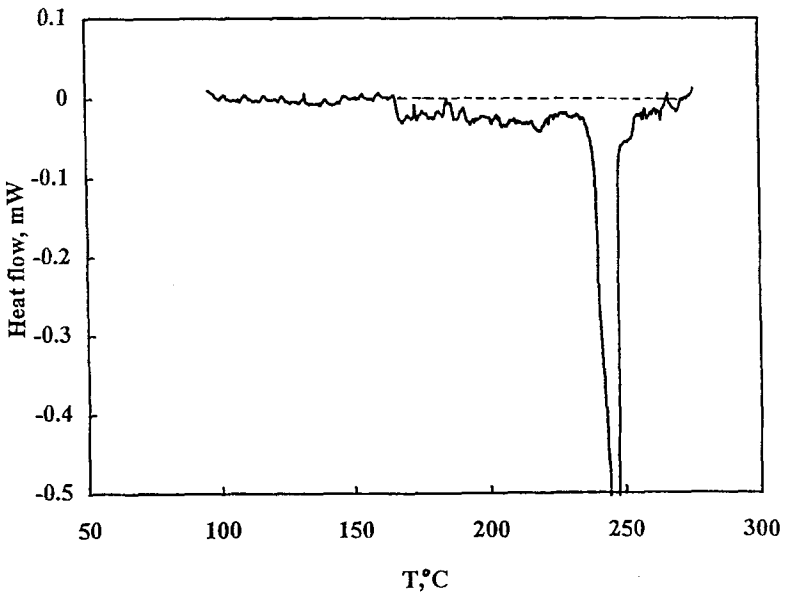

Fig. 4 Melting trace with two melting regions. Recrystallized P4MP, $v=3$ K h^{-1}, $m_p=113.4$ mg. Melting is complete and α_c (H)$=0.75$

$\Delta H_{network}$ and ΔH_{dsc} are respectively 30 and 60 J g^{-1} leading to ΔH_{total} =90 J g^{-1}. About a third of the crystal enthalpy has been evolved below T_m. The results of other experiments are given in Table 2. The separation of ΔH_{total} into ΔH_{dsc} and $\Delta H_{network}$ depends on the conditions of melting. If m_p is smaller and v, the temperature ramp, is faster, the amount of unstrained network is larger. The experiment listed in Table 2 with $m_p=66.5$ mg is such an example. The less strained network starts melting at 129°C and ends at 238°C, so that $\Delta H_{network}$ is equal to 80 J g^{-1} and ΔH_{dsc} to 42 J g^{-1}. Evidently, there are some ambiguities in the separation of the endotherms in case of overlap.

A feature of $\Delta H_{network}$ for P4MP is that the high temperature contribution is small, less than 15 J g^{-1}. For PE, however, it may reach one third of ΔH_{total}. This is a strong indication that the main peak of fusion as it occurs in P4MP is already in equilibrium with a strained melt.

2. Crystallization traces

Figure 5 gives a typical trace for crystallization. The substrate is stainless steel and $m_p=94.9$ mg. The characteristic parameters of the trace and of others are listed in Table 3. Again, one sees two regions of crystallization. The ΔH_{dsc} is 48 J g^{-1} and $\Delta H_{network}$ is 47 J g^{-1}. The temperature range for the integration of $\Delta H_{network}$ overlaps with that of the main crystals. The ΔH_{total} is equal to 95 J g^{-1}

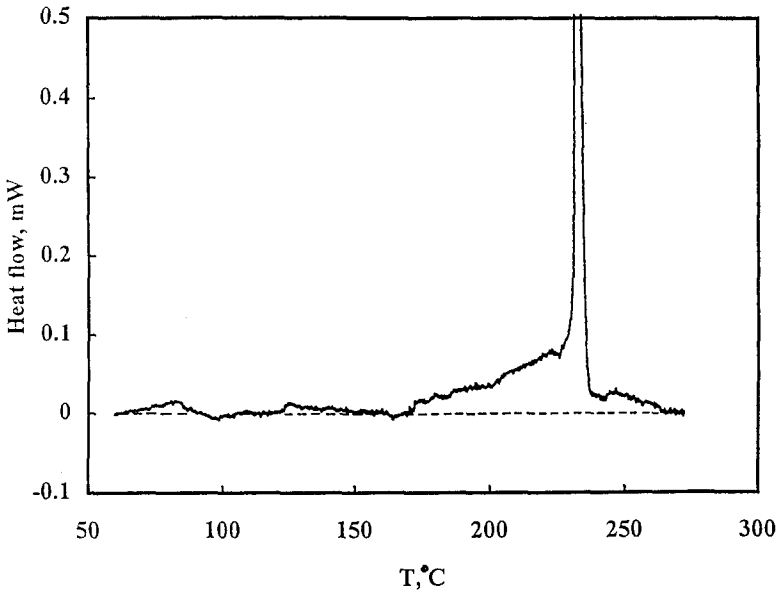

Fig. 5 Crystallization trace with two crystallization regions. $v=3$ K h^{-1} from the melt equilibrated at 280°C, $m_p=94.9$ mg. Crystallization is complete

and equal also to ΔH_{total} for the second melting. In traces recorded down to RT one notices small exotherms (<10 J g^{-1}) between 160 and 50°C which have not been included in the discussion.

3. Fusion of nascent P4MP

Figures 6a and b give examples of the melting trace of nascent P4MP. The substrate is Hg for 6a ($m_p=26.2$ mg) and stainless steel for 6b ($m_p=94.9$ mg). The combination of a slower ramp, presence of substrate and higher mass makes the melting endotherm $\Delta H_{network}$ very clear in Fig. 6b. A region of arrested melting is noted betwen 188 and 201°C. Table 4 lists the characteristics of that trace and of the others and, in particular, the values of ΔH_{total}. The value of ΔH_{total} varies by 30 J g^{-1} depending on the conditions. As found for PE and iPP, smaller amounts of polymer lead to more complete fusion. However, as v itself is changing from 1.2 to 12 K h^{-1}, one cannot generalize any trend on the data found on the table.

4. Effect of substrate

The data in Tables 2 and 4 show no difference between the T_m values of recrystallized and nascent P4MP samples. This has been found also when melting is achieved by fast DSC. This result is different from ultra-high molecular

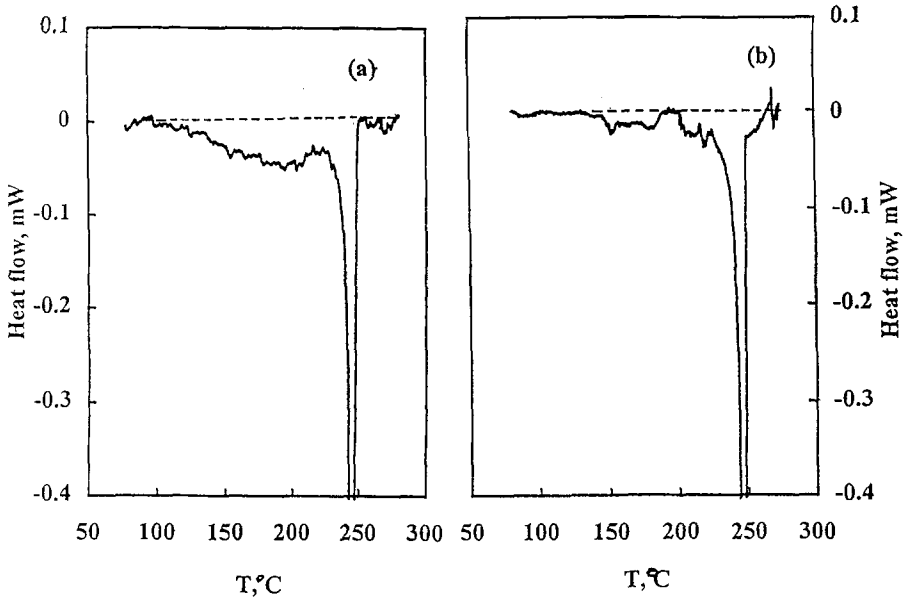

Fig. 6 Melting traces with two melting regions. Nascent P4MP. 6a. $v=12$ K h^{-1}, $m_p=26.2$ mg on Hg. Melting is incomplete. 6b. $v=3$ K h^{-1}, $m_p=94.9$ mg on stainless steel. Melting is complete

weight PE where the lowering of T_m may reach 7 K for the second fusion. This is an indication of strain-melting, as said above. The crystallization temperature depends little on conditions.

Also, the reported T_m hardly depends on the substrate since at 3 K h^{-1}, T_m is 246.7°C by itself and 245.7°C on stainless steel. The ΔH_{dsc} varies as expected, being higher for a slow ramp than for a fast ramp; it is also higher when it melts with a substrate than when alone.

Crystallization without substrate

Two experiments of crystallization and second melting in the absence of a substrate are presented. One notices in the first two rows of Table 3 (giving the characteristics of the crystallization trace), that the values of ΔH_{total} are different by 42 J g^{-1} and the values of T_c by 0.8K. The melting traces of these two samples are given in Figs 7a and b. The traces contain more differences than the crystallization traces. The values of T_m differ by 2.2 K for the 3 K h^{-1} ramp. The value of ΔH_{total} for the sample with $m_p=99.8$ mg is constant between $n=2$ and $n=3$. On the other hand, the sample with $m_p=101.7$ mg increases its ΔH_{total} from 65 to 100 J g^{-1}, but one notes a large exotherm of recrystallization between 110 and 180°C, the enthalpy of which is –70 J g^{-1}. In this experiment, crystallization was incomplete, in spite of the 3 K h^{-1} temperature ramp between

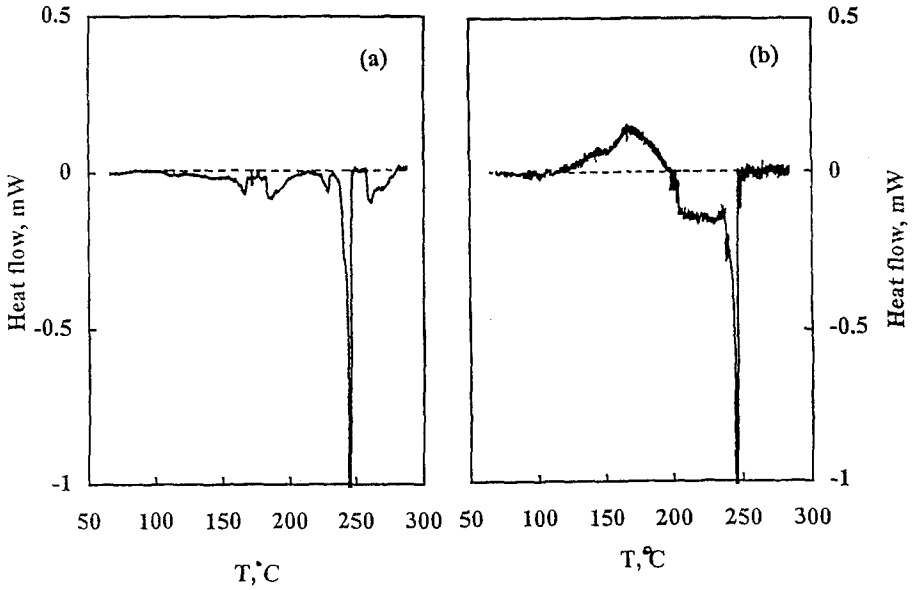

Fig. 7 Effect of a long thermal history on the melting trace; 7a. $v=3$ K h^{-1}, polymer crystallized without substrate, $m_p=99.8$ mg. Melting is complete. 7b. $v=3$ K h^{-1} polymer crystallized without substrate $m_p=101.7$ mg. The fraction melting at low temperature has increased as in Fig. 2c. Exotherm of recrystallization between 110 and 180°C

280 and 60°C. This result is intringuing. It questions the mobility of the non-crystallized chains at the end of the main exotherm of crystallization (230°C). The reason why recrystallization occurs on heating, but not on cooling, is not clear. The crystals grown during the heating ramp melt below the main peak. They have been labelled in Table 2 as network crystals, but their range of melting (198–236°C) is higher than those found in the other traces. They may be crystals melting in equilibrium with a melt which is less strained than that formed when the main crystals are melting at a higher temperature. The conditions of melting and recrystallization of the samples with $m_p=99.8$ and $m_p=101.7$ mg are identical. However, the sample which does not recrystallize has been prepared in a narrower tube (ID=8 mm) under vacuum. The other is placed in a larger tube (ID=13 mm) flushed with N_2. Further work should permit to understand this effect.

5. Analysis of the dissolution traces

Dissolution traces have been taken in different solvents to understand the gel formation. Our aim was to obtain disentangled crystals. The results will be presented later. The traces given here correspond to $n=1$ and $n=3$ (after a slow crystallization at 3 K h^{-1}) of a 1% solution in heptane. The analyses are given

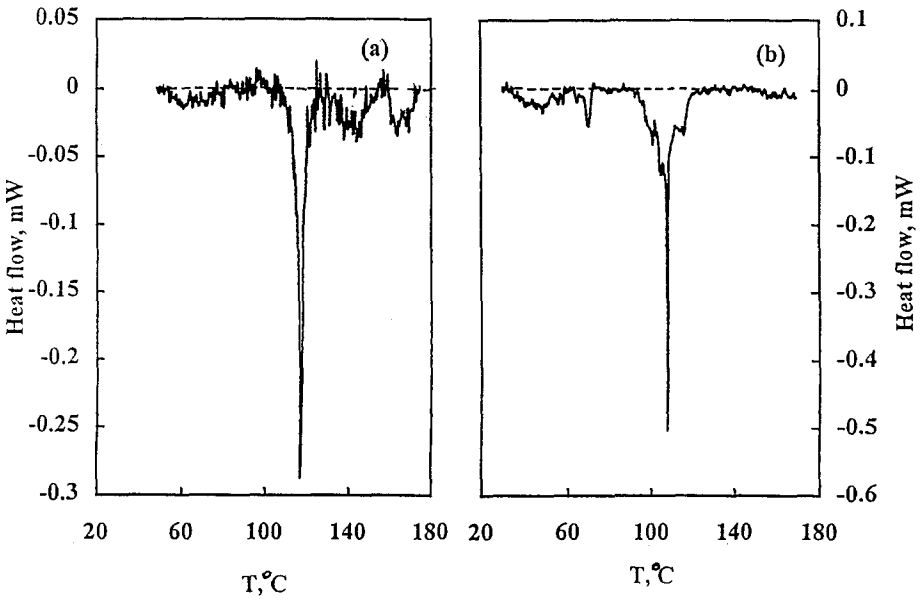

Fig. 8 Dissolution traces with two ranges of dissolution. In *n*-heptane, $c=1.1\%$ showing T_d (calorimeter) and the change in strained dissolution between $n=1$ and $n=3$; 8a. Nascent sample. Part of the polymer undergoes a strained dissolution which ends at 175°C; 8b. Recrystallized crystals. Most of the polymer undergoes a non-strained dissolution which ends at 122°

in Table 5. The value of ΔH_{total} is low but increases by 11 J g^{-1} on slow crystallization. $\Delta H_{network}$ is small. The following points can be made:

i. The end of the main peak is 125°C for the nascent crystals and is well defined. This is the same temperature as found under the microscope.

ii. Another point pertains to the difference in T_d between the dissolution of nascent (117.2°C) and recrystallized crystals (107.6°C). Some relaxation of the melt has taken place during the process, relaxation which does not occur without solvent.

iii. The values forΔH_{total} are incomplete, by 30 or 40 J g^{-1}. In fact, the endotherm of $\Delta H_{network}$ is missing. This result is interpreted as follows: the network crystals dissolved at the temperature during the equilibrium of the calorimeter.

These results are supportive of the non-equilibrium melting, as explained above.

Conclusion

Based on the prior experiments of slow calorimetry for PE and iPP, the present analysis presents a lower limit to the value of ΔH_o for perfect crystals of

Table 5 Characteristics of the dissolution traces of P4MP in *n*-heptane at 3 K h^{-1}

Sample	m_p^a/ mg	*n*	T_d / °C	ΔH_{total} / J g^{-1}	$\Delta H_{network,L-T}$ J g^{-1}	$\Delta H_{network,H-T}$ / J g^{-1}	ΔH_{dsc} / J g^{-1}	Fig.
Nascent	46.1	1	117.2	55	5	23	27	8a
				(I)	(54–83)	(125–175)	(107–125)	
Crystallized	46.1	3	107.6	66	14	0	52	8b
at 3 K h^{-1}				(I)	(34–74)		(91–122)	

[a] Solvent volume is 4 cm^3

P4MP. A value higher or equal to 100 J g^{-1} seems reasonable. This is on the high side of the range of values obtained by other techniques [21].

The slow calorimetry detects about 20 J g^{-1} more enthalpy of fusion which should also contribute to X-ray crystallinity. The value of α_c (H) should thus be equal to about 0.75 (75 J g^{-1}/100 J g^{-1}) and is realistic and comparable to X-ray crystallinity. The effect of melting on a substrate in obtaining the complete melting of a nascent sample, i.e. a high value of $\Delta H_{network}$ and ΔH_{total}, found on iPP and PE, is confirmed.

To explain the failure of the Flory-Huggins equation relating the dissolution temperatures T_d and ΔH_o, it has been hypothezised that T_m for P4MP melts in equilibrium with a strained melt, but dissolves in equilibrium with a relaxed or partially relaxed melt. Justifications of this model are found in the literature and in heats of swelling or of gel-forming. Further work is continuing to extend some of the findings presented in this work.

* * *

The authors benefitted from the last four decades of work in polymer physics by Professor Wunderlich, in particular from the books of Macromolecular Physics which contain extensive and selected information and give insight into the complex behavior of macromolecules. Personal discussions with Prof. Wunderlich reinforced our belief that interesting and unexpected results can happen when simple macromolecules change phase and that these events can be interpreted, at least semi-quantitatively, in terms of non-equilibrium thermodynamics. The authors and younger members of our research group wish Prof. Wunderlich many more years of fruitful research.

We are grateful to Dr P. L. Klegg for his generous shipment of P4MP over the years. P4MP is an ICI product which is prized for its purity and high stereoregularity.

We also acknowledge the support of the National Science and Engineering Research Council of Canada.

References

1 L. C. Lopez, G. L. Wilkes, P. M. Stricklen and S. A. White, Rev. Macromol. Chem. Phys., C32 (3&4) (1992) 301.
2 P. Geil, Polymer Single Crystals. R. E. Krueger Publishing Cie, Huntington NY 1973.
3 G. Natta, P. Corradini and I. N. Bassi, R. C. Acad. Linces., 19 (1955) 404.
4 G. Charlet and G. Delmas, Polymer, 25 (1984) 1619.
5 G. Charlet, G. Delmas, J. F. Revol and R. St. J. Manley, Polymer, 25 (1984) 1613.
6 G. Charlet and G. Delmas, Polym. Bull., 6 (1982) 367.
7 A. Aharoni, G. Charlet and G. Delmas, Macromolecules, 14 (1984) 1613.
8 P. Zoller, J. Appl. Polym. Sci., 21 (1977) 3129.
9 P. Zoller, H. W. Starkweather Jr. and G. A. Jones, J. Polym. Sci., Polym. Phys. Ed., 24 (1986) 1451.
10 C. E. Wilkes and M. H. Lehr, J. Macromol. Sci.-Phys., B7(2) (1973) 225.
11 J. K. Kruger, L. Peetz, M. Pietralla and H. G. Unruh, Polym. Bull., 4 (1981) 591.
12 R. F. Boyer, K. M. Panichella and H. G Unruh, Polym. Bull, 9 (1983) 344.
13 S. Rastogi, M. Newman and A. Keller, Nature, (1991) 53.
14 H. Phuong-Nguyen and G. Delmas, Macromolecules, 28 (1985) 1235.

15 G. Charlet, H. Phuong-Nguyen and G. Delmas, Macromolecules, 17 (1984) 1200.
16 G. Charlet, Ph. D. Thesis, McGill Univ., Dept. Chem., Montreal, Canada (1982).
17 T. Tanigami, H. Suzuki, K. Yamaura and S. Matsuzawa, Macromolecules, 18 (1985) 2595.
18 J. M. Williams and J. E. Moore, Polymer, 28 (1987) 1950.
19 J. M. Williams and J. E. Moore, Polymer, 30 (1989) 2279.
20 J. M. Williams, J. Mater. Sci. 23 (1988) 900.
21 G. Charlet and G. Delmas, J. Polym. Sci., Polym. Phys. Ed., 26 (1988) 111.
22 P. C. Jain, B. Wunderlich and D. R. Chaubey, J. Polym. Sci., Polym. Phys. Ed., 15 (1977) 2271.
23 A. Keller and F.M. Willmouth, Makromol. Chem., 121 (1969) 42.
24 F. de Candia, P. Lanelli, O. Staulo and V. Vittoria, Colloid Polym. Sci., 698 (1988) 266 (7).
25 X. Xhang, I. Lapes, H. Phuong-Nguyen and G. Delmas, submitted to J. Polymer Science Part 1.
26 H. Phuong-Nguyen and G. Delmas, Macromolecules, 25 (1992) 414.
27 H. Phuong-Nguyen and G. Delmas, Macromolecules, 25 (1992) 408.
28 H. Phuong-Nguyen and G. Delmas, J. Materials Sci., 29 (1994) 3612.
29 H. Phoung-Nguyen and G. Delmas, Thermochim. Acta, 238 (1994) 257.
30 H. Phoung-Nguyen and G. Delmas, J. Sol. Chem., 23 (1994) 249.
31 G. Delmas, J. Polym. Sci. Part B: Polym. Phys. Ed., 31 (1993) 2011.
32 F. Rybnikar and P. H. Geil, J. Macromol. Sci.-Phys., B7 (1973) 1.
33 Y. Hase and P. H. Geil, Polym. J., 2 (1971) 560.
34 Y. Hase and P. H. Geil, Polym. J., 2 (1971) 581.
35 Y. Hase and P. H. Geil, Makromol. Chem., 181 (1980) 1551.
36 D. R. Morrow, G. C. Richardson, L. Kleinman and A. E. Woodward, J. Polym. Sci. Phys. Ed. 5 (1967) 493.
37 F. Khoury and J. D. Barnes, J. Res. Natl. Bur. Std., A. Phys. Chem., 76a (1972) 225.
38 A. Nakajima, S. Hayashi and T. Taka, Koloid Z. Z. Polym., 233 (1969) 869.
39 S. B. Eng and A. E. Woudward, J. Macromol. Sci. Phy., B10 (1974) 627.
40 B. Wunderlich, Macromolecular Physics, Academic Press, Vol. 3, 1980.
41 J. Grebowicz, S.-F. Llau and B. Wunderlich, J. Polym. Sci. Polymer Symposium, 71 (1984) 19.